

# Geophysical Research Letters

## RESEARCH LETTER

10.1029/2020GL090458

### Key Points:

- The avalanche behaviors from quasi-static shear of granular materials with different size polydispersity are investigated
- The critical behaviors of granular materials can be tuned by adjusting its size polydispersity
- The effective temperature volatility can be used to explain the tuned criticality of granular gouge

### Supporting Information:

- Supporting Information S1

### Correspondence to:

G. Ma,  
magang630@whu.edu.cn

### Citation:

Ma, G., Zou, Y., Gao, K., Zhao, J., & Zhou, W. (2020). Size polydispersity tunes slip avalanches of granular gouge. *Geophysical Research Letters*, 47, e2020GL090458. <https://doi.org/10.1029/2020GL090458>

Received 22 AUG 2020

Accepted 12 NOV 2020

Accepted article online 16 NOV 2020

## Size Polydispersity Tunes Slip Avalanches of Granular Gouge

Gang Ma<sup>1,2</sup> , Yuxiong Zou<sup>1,2</sup>, Ke Gao<sup>3</sup> , Jidong Zhao<sup>4</sup> , and Wei Zhou<sup>1,2</sup>

<sup>1</sup>State Key Laboratory of Water Resources and Hydropower Engineering Science, Wuhan University, Wuhan, China, <sup>2</sup>Key Laboratory of Rock Mechanics in Hydraulic Structural Engineering of Ministry of Education, Wuhan University, Wuhan, China, <sup>3</sup>Department of Earth and Space Sciences, Southern University of Science and Technology, Shenzhen, China, <sup>4</sup>Department of Civil and Environmental Engineering, The Hong Kong University of Science and Technology, Hong Kong

**Abstract** Granular materials have frequently been used as representations of natural fault gouges. Although they can reproduce proper avalanche behaviors, the universality of the scaling exponent of avalanche size remains debatable. As a core issue in both amorphous plasticity and geophysics, avalanche universality may help reconcile the avalanche behaviors of earthquake and granular materials into the same universality class. We examine numerically the signatures of stress avalanches emerging from quasi-static shear of granular materials with different size polydispersity. A persistent serrated plastic flow phenomenon is observed in our models with varying polydispersity. The stress drop is well defined by a truncated power law distribution  $P(s) \sim s^{-\tau} \exp(-s/s_{\max})$ . The exponent  $\tau$  and cutoff stress drop  $s_{\max}$  show a clear dependence on polydispersity, which reflects a tuned criticality. We further calculate the effective temperature from the statistics of energy fluctuations. The effective temperature volatility can be used to explain the tuned critical behaviors of granular gouge.

**Plain Language Summary** Granular materials are ubiquitous in nature and important to a wide range of industrial processes. When driven at slow rates, granular materials deform via intermittent dynamics which alternates slow elastic loading with rapid slips. Such serrated behaviors have attracted attentions from researchers in material science, process engineering and powder technology. They have aroused great interest for geoscientists since key clues may be offered for the origin of earthquake physics. The avalanche-like slip events of granular materials reveal a strong statistical similarity with earthquakes, having made granular materials widely adopted as an ideal laboratory model material for the study of earthquake physics. Different granular systems subjected to different loading conditions present similar scaling laws, such as the power law distributions of event size. However, the scaling exponents describing avalanche distributions vary greatly in range, posing challenges to the existence of universal scaling across diverse granular systems. In this study, we examined granular systems with varying size polydispersity from monosized spheres to highly polydisperse packings and found the signature of tunable avalanche statistics. We further use size polydispersity as a control parameter to generate continuously adjustable avalanche statistics.

## 1. Introduction

Earthquakes are among the most catastrophic events in nature. The magnitude of an earthquake,  $M$ , has been found to show interesting scale-free statistics (Gutenberg & Richter, 1954). The number of earthquake  $N$  with magnitude larger than  $m$  can be approximately expressed by the Gutenberg-Richter law  $\log_{10} N(M > m) \propto -bm$ , where  $b$  is a positive constant with a value around one (Bak et al., 2002; Schofield & Wroth, 1968). The empirical law is consistent with the power law distribution of energy release  $P(E) \propto E^{-\tau}$ , where  $\tau = 1 + \frac{2}{3}b$ . The exponent  $\tau$  varies in a range depending on the considered earthquake catalog and region (Batac et al., 2017; Geller et al., 2015; Kagan, 2002; Marković & Gros, 2014; Nicolas et al., 2018). Understanding earthquake dynamics, especially the origin of scale-free statistics, remains a major issue in geophysics.

In addition to earthquake events, the intermittent dynamics and scale-free avalanches have also been observed from a broad range of amorphous solids, such as rocks and porous media (Barés et al., 2018; Baró et al., 2013), and granular materials (Barés et al., 2017; Denisov et al., 2016; Murphy et al., 2019),

when driven at slow rates. Particularly, it has been found that granular materials can reproduce realistic seismicity laws and rheological behaviors when it is slowly sheared upon yielding. In further view of its structural similarity to earthquake gouges, granular materials have become a promising model system for studying earthquake physics (Daniels & Hayman, 2008; Gao et al., 2019, 2020; Kumar et al., 2020; Lherminier et al., 2019; Michlmayr et al., 2013).

Among the reported experimental studies designed to characterize the avalanche statistics in deformed granular solids (Abed Zadeh et al., 2019; Barés et al., 2017; Denisov et al., 2016; Kumar et al., 2020; Lherminier et al., 2019; Murphy et al., 2019), the avalanche size exponent was found ranging from 1.2 to 1.7, showing a considerable scatter. The cutoff value of avalanche size also shows a clear stress dependency (Denisov et al., 2016; Friedman et al., 2012; Gao et al., 2018; Rivière et al., 2018) and particle shape dependency (Murphy et al., 2019) and is dependent on the particle friction and packing fraction (Barés et al., 2017). Statistical physics indicates that the scaling law and the value of critical exponent govern the universality class in which a system belongs to. The universality hypothesis is appealing since various physical systems following the equivalent scaling law and sharing the value of critical exponent can be grouped into the same universality class (Marković & Gros, 2014; Ostojic et al., 2006). It is readily realized that one can tune the critical behavior of granular materials to quantitatively reproduce most of the scaling behaviors of earthquakes without having to include their microscopic details.

Among various potential regulation means, loading conditions and material properties have rather marginal effects on the avalanche statistics (Budrikis et al., 2017; Kumar et al., 2020). Granular assemblies composed of particles of different shapes can generate different avalanche statistics (Murphy et al., 2019). The overall form and local edges and corners of particles may influence the slip avalanches in different manners. Most natural granular materials are polydisperse, consisting of a wide range of particle sizes (Lai et al., 2017). The effects of particle shape on granular materials is significant only at low size polydispersity where the short-range positional and/or orientational order dominates (Nguyen et al., 2014). Therefore, the size polydispersity may play a more important role in slip avalanches.

We present in this letter the avalanche behaviors that emerged from quasi-static shear of granular materials with different size polydispersity. We use 3-D discrete element method to simulate the slow shearing of granular assemblies from their initial states to the critical state (a state featured by constant volume and constant stress). We then perform the statistics on avalanche size and relate the slip event to the system and particle-scale energy fluctuations and nonaffine displacements. Finally, we explain the size polydispersity dependence of slip avalanche in terms of effective temperature fluctuation.

## 2. Materials and Methods

Slow shearing of granular materials has been widely used to generate laboratory-scale earthquakes (Daniels & Hayman, 2008; Dorostkar et al., 2017a, 2017b; Ferdowsi et al., 2014, 2018; Johnson et al., 2013; Lieou et al., 2015). We model the granular materials as an assembly of spheres with prescribed particle size distribution (PSD) (see Text S1 and Figure S1 in the supporting information). By using different PSDs, we control the size polydispersity of the system, which defines the degree of polydispersity as the standard deviation of particle sizes  $\Delta = \sqrt{(\langle d_p^2 \rangle - \langle d_p \rangle^2) / \langle d_p \rangle}$ , where  $d_p$  denotes the particle diameter and  $\langle \cdot \rangle$  denotes the ensemble average over all particles.

We simulate the simple shearing of granular materials using LIGGGHTS (Kloss et al., 2012), an open-source discrete element code that has been well validated and verified. The model setup is shown in Figure 1a in which a rectangular solid domain is employed. The sizes in the three directions are respectively  $40 \bar{d}$  (length)  $\times 20 \bar{d}$  (depth)  $\times 10 \bar{d}$  (height), where  $\bar{d}$  is 0.001 m (see Text S2 for the selection of sample height). The granular systems are compressed and sheared by two rough particle walls, which are composed of spherical bonded particles with diameters uniformly distributed within  $[0.9, 1.1]\bar{d}$ . The granular assemblies are first compressed to the prescribed normal pressure  $p = 10$  MPa. The bottom wall is then moved in the shear direction with a constant velocity while keeping the vertical movement constrained. The top wall is fixed in the shear direction and the normal pressure is maintained constant by servo control. The shear rate, defined as the ratio of shear velocity to the undeformed sample height, is set to  $\dot{\gamma} = 0.1$ . This

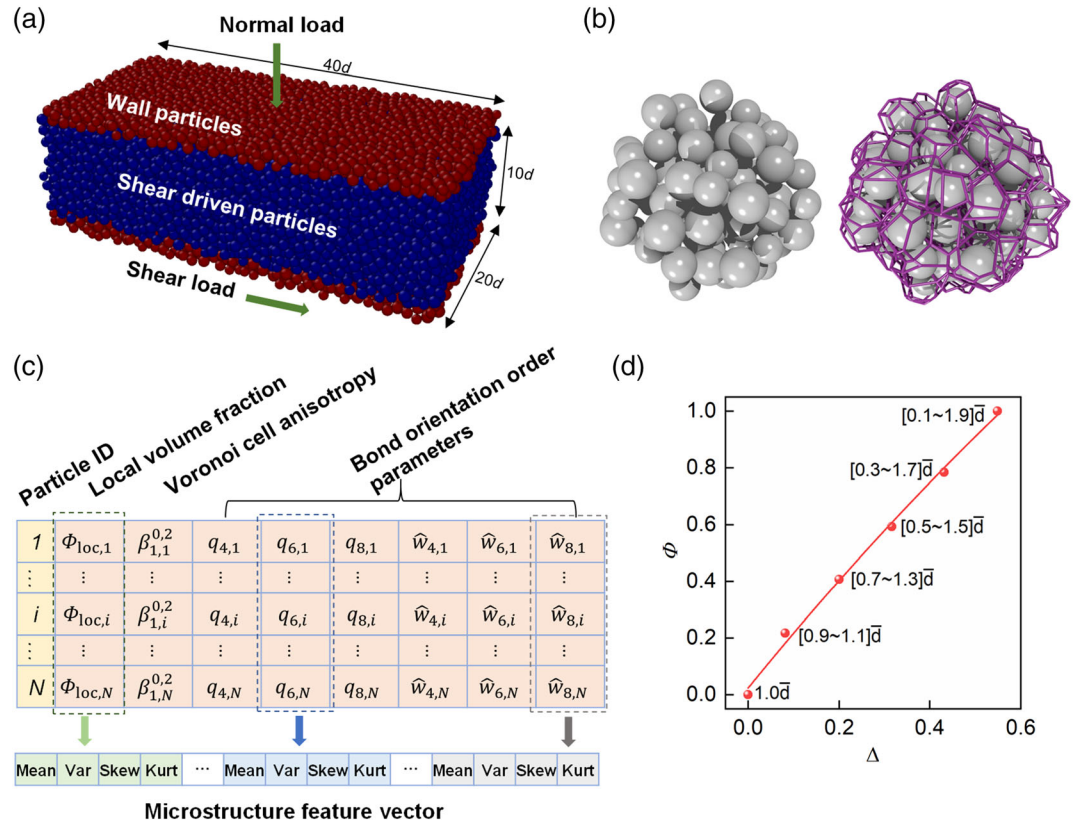


**Figure 1.** (a) Schematic of the model setup. Normal pressure and shear displacement are applied on the top and bottom walls, respectively. Periodic boundary conditions are applied in the shear and depth directions. (b) Illustration of Voronoi tessellation of a particle assembly using Voro++ (Rycroft, 2009). (c) We calculate the particle level order parameters and calculate their statistics (mean, variance, skewness, and kurtosis). These statistical features are then concatenated as a feature vector representing the structural characteristics of the granular system (Wang & Jain, 2019). (d) Relationship between the size polydispersity  $\Delta$  and the reduced indicator of structural characteristics  $\phi$ .

shear rate yields an inertia number  $I = \dot{\gamma} \bar{d} / \sqrt{p/\rho} \approx 10^{-6}$  ( $\rho$  is the particle density) for the system, which is small enough to guarantee a quasi-static regime (Ferdowsi et al., 2015; Midi, 2004). The small shear rate is slow enough to ensure that individual avalanches can be identified to avoid avalanche overlap. The stable time increment for the digital elevation model (DEM) simulation is  $\Delta t_{\text{stable}} = 1 \times 10^{-8}$  s.

The particles are considered deformable and interact with one another through the Hertz-Mindlin contact model with Coulomb sliding friction. The particles have a density of  $2,900 \text{ kg/m}^3$ , Poisson's ratio of 0.25, Young's modulus of 65 GPa, friction coefficient of 0.1, and restitution coefficient of 0.87. This set of parameters are often used in the DEM simulations of granular fault gouge (Dorostkar et al., 2017a, 2017b). The wall particles adopt the same material properties as those in the shear body. The friction coefficient between the particle walls and the shear body is set to 0.9 to enhance surface friction (Dorostkar et al., 2017b).

The introduction of size polydispersity has a pronounced effect on the structural properties of the granular system. We calculate the structural order parameters of each particle based on analyses of the Voronoi tessellations (Figure 1b). We obtain eight vectors (corresponding to eight structural order parameters shown in Figure 1c and defined in Text S3) whose length is the number of particles. By computing the statistical features of each order parameters, for example, mean, variance, skewness, and kurtosis, we obtain a feature vector of length 32 containing the structural information of each granular system (Figure 1c). Finally, we extract a single measure representing the structural characteristics from the feature vector using the  $t$ -SNE technique (Varoquaux et al., 2015). As seen in Figure 1d, the granular systems with different degrees of polydispersity have distinct structural characteristics.

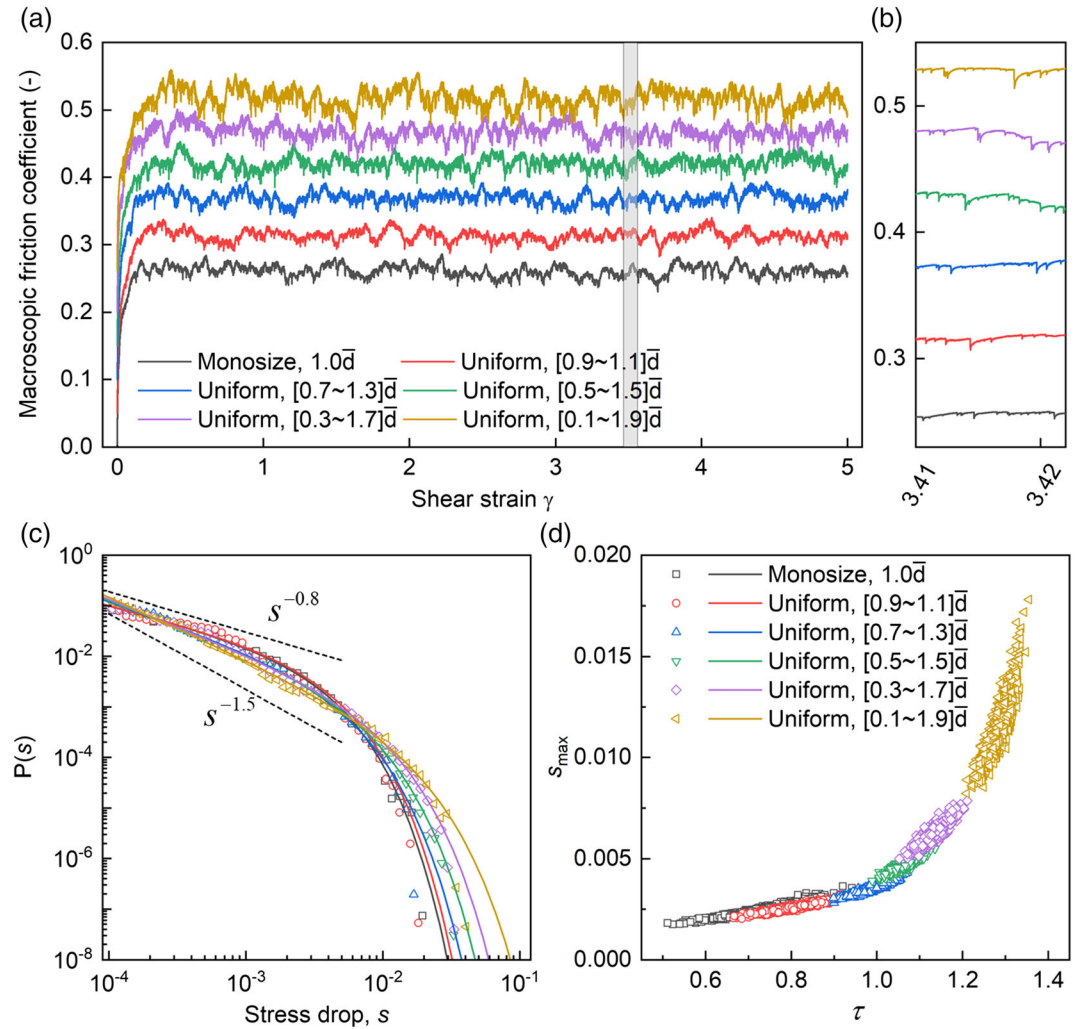


**Figure 2.** (a) Stress-strain curves of six granular systems. The y axis denotes the shear stress  $\sigma$  normalized by the normal pressure  $p$ . The curves have been shifted vertically by 0.1 to facilitate visualization. (b) Enlarged view of the gray box indicated in Figure 2a. (c) Probability distributions of stress drop  $P(s)$  for different systems. The solid lines are truncated power law fits to the data. (d) Parameter space for the truncated power law fits to  $P(s)$ .

### 3. Results

#### 3.1. Slip Avalanche Statistics

To generate enough data for statistical analysis, we shear the granular system up to a shear strain  $\gamma = 5.5$ . The data are extracted every  $1 \times 10^{-5}$  shear strain for further analysis. The effects of size polydispersity on the mechanical responses of granular materials is illustrated by the stress-strain curves shown in Figure 2a. The macroscopic friction coefficient is defined as the ratio of the shear stress to the normal pressure. The overall response shows an initial nonlinear elastic increase up to the onset of yielding before gradually transiting a regime referred to as critical state in soil mechanics. At this state, the granular system shows serrated stress fluctuations consisting of a sudden stress drop followed by nonlinear stress recovery after each event. The serrated plastic flow discussed in this study is extracted from the stress-strain data in the critical state past yielding, that is,  $0.5 \leq \gamma \leq 5.5$ . This ensures a wide range of predicted scaling exponents and scaling functions to identify the underlying slip statistics and dynamics.

Figure 2b shows a magnification of the stress-strain curves for  $\gamma$  ranging from 3.410 to 3.422. It shows clearly that both the magnitude of stress drop is larger, and the shape of serration becomes sharpened with the increase of size polydispersity. Figure 2c presents the statistical distributions of avalanche size  $s$ , that is,

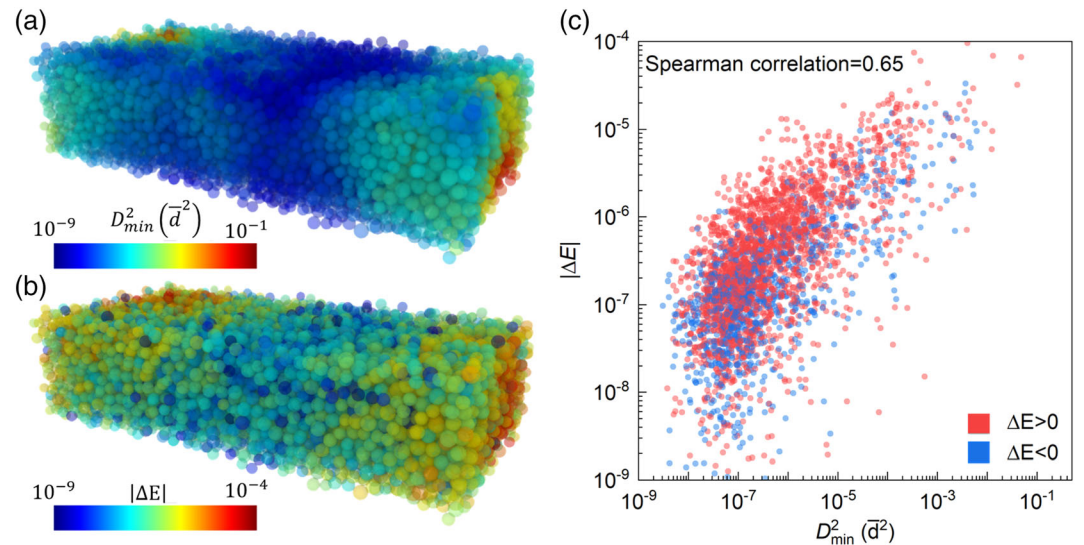


**Figure 3.** The spatial maps of energy fluctuations  $|\Delta E|$  in (a) and nonaffine displacements  $D_{\min}^2$  in (b). The data are obtained during a slip event of size  $s = 0.0157$  and strain duration  $\delta\gamma = 3 \times 10^{-5}$ . Note that the wall particles are not presented. (c) Correlation between  $D_{\min}^2$  and  $|\Delta E|$ .

the magnitude of stress drop. The stress drop data are plotted logarithmically. Larger stress drops are more probable as the system size polydispersity increases, which is consistent with the serrations depicted in Figure 2b.

Similar to what has been reported for other slow shear of granular materials (Denisov et al., 2016; Murphy et al., 2019), we find the probability distributions of stress drop  $P(s)$  are well fitted by a truncated power law  $P(s) \sim s^{-\tau} \exp(-s/s_{\max})$ . The cutoff  $s_{\max}$  describes the maximum size of avalanches. The exponent  $\tau$  of the power law is considered to tell about the mechanism leading to scale-free dynamics (Murphy et al., 2019). Uncertainty of the data fitting was estimated using the bootstrap method. We resampled the stress drop data 1,000 times and then fitted the resampled drop distribution. Figure 2d shows the parameter space for the truncated power law fits to  $P(s)$ . Both the exponent  $\tau$  and the cutoff stress drop  $s_{\max}$  show strong polydispersity dependency.  $s_{\max}$  increases nonlinearly with polydispersity and varies over 1–2 orders of magnitude. The exponent  $\tau$  also shows a clear increasing tendency with polydispersity and covers a range between 0.6 and 1.5. Despite the significant variations, both  $\tau$  and  $s_{\max}$  have a clear scaling relation across a board range of size polydispersity.

### 3.2. Particle Level Energy Fluctuations

According to amorphous plasticity, the serrated flow is attributed to the localized plastic zones undergoing irreversible rearrangements and their long-range interactions through elasticity (Denisov et al., 2016; Leishangthem et al., 2017; Ma et al., 2021; Niiyama et al., 2019). The most significant drops often result from the localized plastic zones that would span the entire system. The slip avalanche can also be interpreted from the perspective of stick-slip dynamics (Daniels & Hayman, 2008; Gao et al., 2018; Michlmayr et al., 2013; Tordesillas et al., 2014). The strong correlations between the stress drop, the system potential energy drop, and the plastic activity size (see Text S6 and Figures S3 and S4) indicate that the localized plastic activity and stick-slip dynamics are essentially related. We calculate the particle-scale energy fluctuation  $\Delta E_i = E_i(\gamma + \Delta\gamma) - E_i(\gamma)$  and nonaffine displacements  $D_{i, \min}^2$  over the strain interval  $\Delta\gamma$  for each particle  $i$ , where  $E_i$  is calculated by summing all the work done to deform the particle  $i$ . Details of the calculation are provided in Texts S4 and S5.

Figures 3a and 3b show that the spatial maps of  $|\Delta E|$  and  $D_{\min}^2$  occurred during a large slip event. These two particle-scale measures show a significant correlation. At very small temporal scales, both energy fluctuations and nonaffine motion are attributed to the evolution of contact force network. Due to the fragility of contact force network and short lifespans of strong force chains, the hot spots with intense energy fluctuations and nonaffine motion are more inclined to originate from particles experiencing large stick-slip

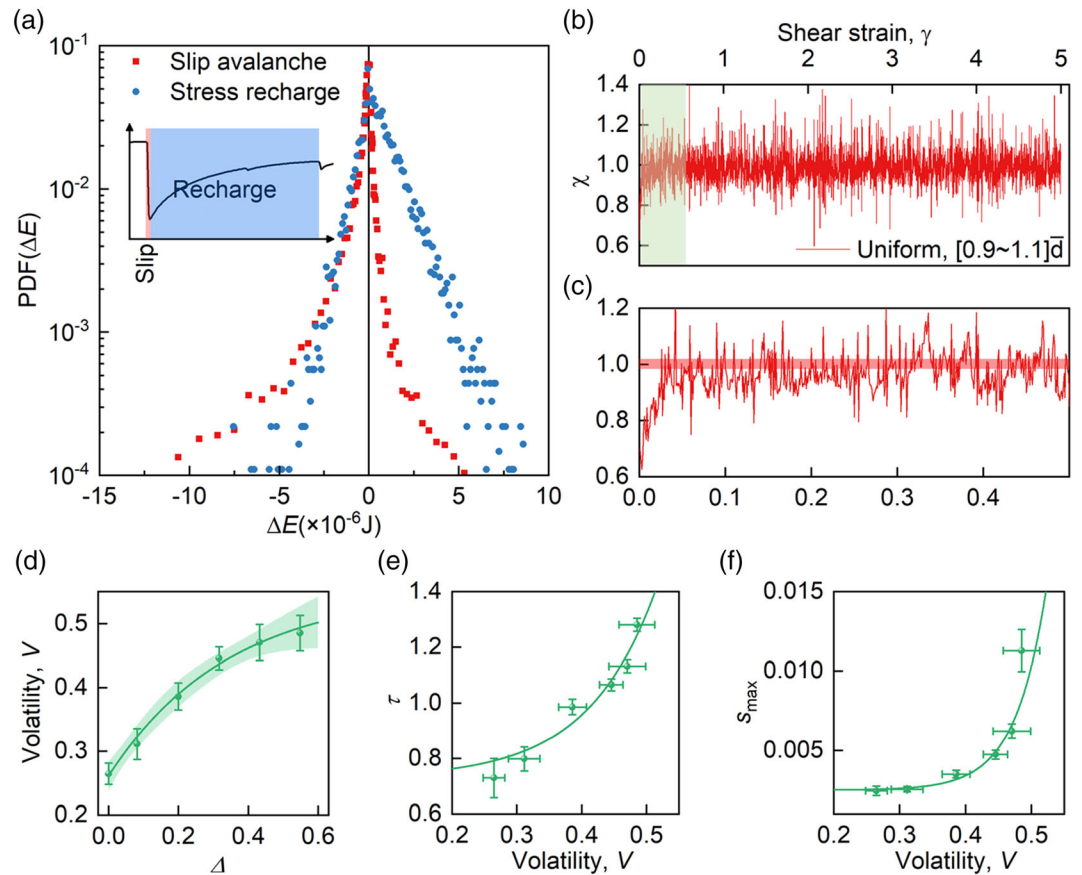


**Figure 4.** (a) Probability distribution functions of energy fluctuations  $\Delta E$  during a slip event and its subsequent recharge (depicted in the inset). (b) Evolution of the effective temperature  $\chi$  of a slightly polydisperse granular system. (c) Enlargement of box region in Figure 4b. (d) The exponential decay relation between size polydispersity  $\Delta$  and effective temperature volatility  $V$ . The error bars are calculated by dividing the  $\chi$  data series into ten equal parts. (e) Exponential growth relation between volatility  $V$  and power law exponent  $\tau$ . (f) Exponential growth relation between volatility  $V$  and cutoff stress drop  $s_{\max}$ . The error bars of  $\tau$  and  $s_{\max}$  are obtained from Figure 2d.

fluctuations (Tordesillas et al., 2016). The correlation does not show a significant difference for  $\Delta E > 0$  and  $\Delta E < 0$ , as both contact establishment and breakdown could lead to changes in the surrounding force network environment and nonaffine motion. Moreover, the correlation does not extend to a large temporal scale since particles have typically experienced several stick-slip fluctuations before this limit, and the nonaffine motion is manifested as irreversible particle rearrangements.

This observation, in conjunction with the previous studies on stick-slip dynamics, raises an interesting question on how to characterize stick-slip fluctuations. As the positive and negative energy fluctuation is related to the stiffening and weakening of the local environment for a particle, clues may be found from the statistics of  $\Delta E$  for gouge dynamics. The probability distribution functions (PDF) of  $\Delta E$  during the slip event (demonstrated in Figure 3) and the subsequent recharge stage are shown in Figure 4a. For both stages, the PDF of  $\Delta E$  shows an asymmetric double-exponential distribution, that is,  $\text{PDF}(\Delta E > 0) \sim \exp(-|\Delta E|/\alpha_+)$  and  $\text{PDF}(\Delta E < 0) \sim \exp(-|\Delta E|/\alpha_-)$ , where  $\alpha_+ \neq \alpha_-$ . The asymmetric feature of the PDF is consistent with the increase ( $\alpha_- < \alpha_+$ ) and drop ( $\alpha_- > \alpha_+$ ) of the system potential energy during the stick-slip cycles. The cause of the double-exponential distribution of  $\Delta E$  has yet to be fully understood. The shear experiment by Zheng et al. (2018) unveiled that the energy fluctuations may be a result of random excitations of force chains (Geng & Behringer, 2005).

By fitting the  $\text{PDF}(\Delta E < 0) \sim \exp(-|\Delta E|/\alpha_-)$  and  $\text{PDF}(\Delta E > 0) \sim \exp(-|\Delta E|/\alpha_+)$  in strain interval  $\Delta\gamma$  at every strain  $\gamma$ , we can get two energy scales of  $\alpha_{\pm}(\gamma)$ . Further, we calculate the effective temperature defined as  $\chi = \alpha_-/\alpha_+$ , which gives is a dimensionless measure of the competition between the

shear-induced strengthening and weakening in terms of particle potential energy (Zheng et al., 2018). Although defined in different manners, the effective temperature used in this study and the granular temperature (see Text S7) defined in terms of the particle velocity fluctuations are both based on thermodynamics theory (Ma et al., 2018; Ma et al., 2019; Zhao & Crosta, 2018). As shown in Figures 4b and 4c, at the beginning of shearing, the primary trend of particle potential energy is growing and  $\alpha$  is systematically below  $\alpha_+$ , leading to  $\chi < 1$ . After further shearing, the values of  $\alpha$  and  $\alpha_+$  becomes comparable, and thus,  $\chi$  first approaches one near the yield strain and then fluctuates around this value.

We then quantify the “temporal” fluctuation of effective temperature in terms of volatility. The volatility of

$\chi(\gamma)$  is given by  $V = \sqrt{\frac{1}{N-1} \sum_{i=1}^N (R_i - \bar{R})^2}$ , where  $N$  is the number of strain intervals,  $R_i = \ln(\chi_i/\chi_{i-1})$  and the subscript  $i$  denotes the location of data in the series. The strain interval  $\Delta\gamma$  between measurements  $\chi_{i-1}$  and  $\chi_i$  is set to  $10^{-4}$ . A volatility value of  $10^{-2}$  indicates that the effective temperature fluctuation is on the scale of 1% of the average value. Figure 4d reveals that the effective temperature volatility  $V$  increases very rapidly with size polydispersity  $\Delta$  at first, and then level off to become asymptotic to the upper limit. This indicates that the macroscopic response of a granular system with higher polydispersity is controlled by a more violent effective temperature fluctuation. Figures 4e and 4f further demonstrate that both  $\tau$  and  $s_{\max}$  show exponential growth with the increase of  $V$ . A recent experimental study reveals the competition between mechanical stability and entropy in sheared granular materials (Sun et al., 2020). By increasing the interparticle friction coefficient in that study and the size polydispersity in the present work, the effect of entropy will dominate and lead to a stronger competition between the strengthening and weakening of energy fluctuations.

#### 4. Conclusions

We investigated the avalanche behavior of granular materials with different size polydispersity. The ubiquitous of serrated plastic flow and power law distributed avalanche size implies that the discrete nature of granular systems is intrinsically responsible for slip avalanche. Although the avalanche size distributions follow the same scaling functions (i.e., truncated power law), they have different exponent  $\tau$  and cutoff stress drop  $s_{\max}$ , indicating a polydispersity-dependent avalanche statistics. The exponent  $\tau$  covers a range of 0.6–1.5 and  $s_{\max}$  varies over 1–2 orders in magnitude. The large tunability renders granular materials an attractive model system for the study of earthquake physics. We can regulate the critical behaviors of granular materials by adjusting its size polydispersity.

To exact the polydispersity dependency in a model-free manner, we calculated the effective temperature based on the statistics of energy fluctuations. We showed that correlating the volatility of effective temperature with the avalanche statistics provides a powerful tool to quantitatively connect the serrated behavior to the microscopic processes of earthquake gouge. We believe that a more fundamental interpretation of the size polydispersity-dependent avalanche statistics is still required in further study.

#### Data Availability Statement

The data supporting this paper can all be found at the corresponding author's figshare repository ([https://figshare.com/articles/dataset/Size\\_polydispersity\\_tunes\\_slip\\_avalanches\\_of\\_granular\\_gouge/12845150](https://figshare.com/articles/dataset/Size_polydispersity_tunes_slip_avalanches_of_granular_gouge/12845150)).

#### Acknowledgments

We acknowledge the financial support from the National Natural Science Foundation of China (Grant Nos. 51825905, U1865204, and 51779194) and Science project of China Huaneng Group Co. Ltd (HNKJ18-H26). The numerical calculations in this work have been done on the supercomputing system in the Supercomputing Center of Wuhan University.

#### References

- Abed Zadeh, A., Barés, J., Socolar, J. E. S., & Behringer, R. P. (2019). Seismicity in sheared granular matter. *Physical Review E*, 99(5). <https://doi.org/10.1103/PhysRevE.99.052902>
- Bak, P., Christensen, K., Danon, L., & Scanlon, T. (2002). Unified scaling law for earthquakes. *Physical Review Letters*, 88(17), 4. <https://doi.org/10.1103/PhysRevLett.88.178501>
- Barés, J., Dubois, A., Hattali, L., Dalmas, D., & Bonamy, D. (2018). Aftershock sequences and seismic-like organization of acoustic events produced by a single propagating crack. *Nature Communications*, 9(1), 1253. <https://doi.org/10.1038/s41467-018-03559-4>
- Barés, J., Wang, D., Wang, D., Bertrand, T., O'Hern, C. S., & Behringer, R. P. (2017). Local and global avalanches in a two-dimensional sheared granular medium. *Physical Review E*, 96(5), 1–13. <https://doi.org/10.1103/PhysRevE.96.052902>
- Baró, J., Corral, Á., Illa, X., Planes, A., Salje, E. K. H., Schranz, W., et al. (2013). Statistical similarity between the compression of a porous material and earthquakes. *Physical Review Letters*, 110(8), 088702. <https://doi.org/10.1103/PhysRevLett.110.088702>
- Batac, R. C., Paguirigan, A. A., Tarun, A. B., & Longjas, A. G. (2017). Sandpile-based model for capturing magnitude distributions and spatiotemporal clustering and separation in regional earthquakes. *Nonlinear Processes in Geophysics*, 24(2), 179–187. <https://doi.org/10.5194/npg-24-179-2017>

- Budrikis, Z., Castellanos, D. F., Sandfeld, S., Zaiser, M., & Zapperi, S. (2017). Universal features of amorphous plasticity. *Nature Communications*, 8(1), 1–10. <https://doi.org/10.1038/ncomms15928>
- Daniels, K. E., & Hayman, N. W. (2008). Force chains seismogenic faults visualized with photoelastic granular shear experiments. *Journal of Geophysical Research*, 113, B11411. <https://doi.org/10.1029/2008JB005781>
- Denisov, D., Lörincz, K., Uhl, J. T., Dahmen, K. A., & Schall, P. (2016). Universality of slip avalanches in flowing granular matter. *Nature Communications*, 7, 10641. <https://doi.org/10.1038/ncomms10641>
- Dorostkar, O., Guyer, R. A., Johnson, P. A., Marone, C., & Carmeliet, J. (2017a). On the micromechanics of slip events in sheared, fluid-saturated fault gouge. *Geophysical Research Letters*, 44, 6101–6108. <https://doi.org/10.1002/2017GL073768>
- Dorostkar, O., Guyer, R. A., Johnson, P. A., Marone, C., & Carmeliet, J. (2017b). On the role of fluids in stick-slip dynamics of saturated granular fault gouge using a coupled computational fluid dynamics-discrete element approach. *Journal of Geophysical Research: Solid Earth*, 122, 3689–3700. <https://doi.org/10.1002/2017JB014099>
- Ferdowsi, B., Griffa, M., Guyer, R. A., Johnson, P. A., Marone, C., & Carmeliet, J. (2014). Three-dimensional discrete element modeling of triggered slip in sheared granular media. *Physical Review E - Statistical, Nonlinear, and Soft Matter Physics*, 89(4), 1–12. <https://doi.org/10.1103/PhysRevE.89.042204>
- Ferdowsi, B., Griffa, M., Guyer, R. A., Johnson, P. A., Marone, C., & Carmeliet, J. (2015). Acoustically induced slip in sheared granular layers: Application to dynamic earthquake triggering. *Geophysical Research Letters*, 42, 9750–9757. <https://doi.org/10.1002/2015GL066096>
- Ferdowsi, B., Ortiz, C. P., & Jerolmack, D. J. (2018). Glassy dynamics of landscape evolution. *Proceedings of the National Academy of Sciences of the United States of America*, 115(19), 4827–4832. <https://doi.org/10.1073/pnas.1715250115>
- Friedman, N., Jennings, A. T., Tsekenis, G., Kim, J. Y., Tao, M., Uhl, J. T., et al. (2012). Statistics of dislocation slip avalanches in nanosized single crystals show tuned critical behavior predicted by a simple mean field model. *Physical Review Letters*, 109(9), 095507. <https://doi.org/10.1103/PhysRevLett.109.095507>
- Gao, K., Euser, B. J., Rougier, E., Guyer, R. A., Lei, Z., Knight, E. E., et al. (2018). Modeling of stick-slip behavior in sheared granular fault gouge using the combined finite-discrete element method. *Journal of Geophysical Research: Solid Earth*, 123, 5774–5792. <https://doi.org/10.1029/2018JB015668>
- Gao, K., Guyer, R., Rougier, E., Ren, C. X., & Johnson, P. A. (2019). From stress chains to acoustic emission. *Physical Review Letters*, 123(4), 048003. <https://doi.org/10.1103/PhysRevLett.123.048003>
- Gao, K., Guyer, R. A., Rougier, E., & Johnson, P. A. (2020). Plate motion in sheared granular fault system. *Earth and Planetary Science Letters*, 548(July), 1–20. <https://doi.org/10.1016/j.epsl.2020.116481>
- Geller, D. A., Ecke, R. E., Dahmen, K. A., & Backhaus, S. (2015). Stick-slip behavior in a continuum-granular experiment. *Physical Review E - Statistical, Nonlinear, and Soft Matter Physics*, 92(6), 2–6. <https://doi.org/10.1103/PhysRevE.92.060201>
- Geng, J., & Behringer, R. P. (2005). Slow drag in two-dimensional granular media. *Physical Review E - Statistical, Nonlinear, and Soft Matter Physics*, 71(1), 1–19. <https://doi.org/10.1103/PhysRevE.71.011302>
- Gutenberg, B., & Richter, C. F. (1954). *Seismicity of Earth and associated phenomenon* (2nd ed.). Princeton, NJ: Princeton University Press.
- Johnson, P. A., Ferdowsi, B., Kaproth, B. M., Scuderi, M., Griffa, M., Carmeliet, J., et al. (2013). Acoustic emission and microslip precursors to stick-slip failure in sheared granular material. *Geophysical Research Letters*, 40, 5627–5631. <https://doi.org/10.1002/2013GL057848>
- Kagan, Y. Y. (2002). Modern California earthquake catalogs and their comparison. *Seismological Research Letters*. <https://doi.org/10.1785/gssrl.73.6.921>
- Kloss, C., Goniva, C., Hager, A., Amberger, S., & Pirker, S. (2012). Models, algorithms and validation for opensource DEM and CFD-DEM. *Progress in Computational Fluid Dynamics*, 12(2–3), 140–152. <https://doi.org/10.1504/PCFD.2012.047457>
- Kumar, P., Korkolis, E., Benzi, R., Denisov, D., Niemeijer, A., Schall, P., et al. (2020). On interevent time distributions of avalanche dynamics. *Scientific Reports*, 10(1), 1–11. <https://doi.org/10.1038/s41598-019-56764-6>
- Lai, Z., Vallejo, L. E., Zhou, W., Ma, G., Espitia, J. M., Caicedo, B., & Chang, X. (2017). Collapse of granular columns with fractal particle size distribution: Implications for understanding the role of small particles in granular flows. *Geophysical Research Letters*, 44, 12,181–12,189. <https://doi.org/10.1002/2017GL075689>
- Leishangthem, P., Parmar, A. D. S., & Sastry, S. (2017). The yielding transition in amorphous solids under oscillatory shear deformation. *Nature Communications*, 8(1), 1–8. <https://doi.org/10.1038/ncomms14653>
- Lherminier, S., Planet, R., Vehel, V. L. D., Simon, G., Vanel, L., Måløy, K. J., & Ramos, O. (2019). Continuously sheared granular matter reproduces in detail seismicity laws. *Physical Review Letters*, 122(21), 218501. <https://doi.org/10.1103/PhysRevLett.122.218501>
- Lieou, C. K. C., Elbanna, A. E., Langer, J. S., & Carlson, J. M. (2015). Stick-slip instabilities in sheared granular flow: The role of friction and acoustic vibrations. *Physical Review E - Statistical, Nonlinear, and Soft Matter Physics*, 92(2), 1–13. <https://doi.org/10.1103/PhysRevE.92.022209>
- Ma, G., Regueiro, R. A., Zhou, W., & Liu, J. (2019). Spatiotemporal analysis of strain localization in dense granular materials. *Acta Geotechnica*, 14(4), 973–990. <https://doi.org/10.1007/s11440-018-0685-y>
- Ma, G., Regueiro, R. A., Zhou, W., Wang, Q., & Liu, J. (2018). Role of particle crushing on particle kinematics and shear banding in granular materials. *Acta Geotechnica*, 13(3), 601–618. <https://doi.org/10.1007/s11440-017-0621-6>
- Ma, G., Zou, Y., Chen, Y., Tang, L., Ng, T. t., & Zhou, W. (2021). Spatial correlation and temporal evolution of plastic heterogeneity in sheared granular materials. *Powder Technology*, 378, 263–273. <https://doi.org/10.1016/j.powtec.2020.09.053>
- Marković, D., & Gros, C. (2014). Power laws and self-organized criticality in theory and nature. *Physics Reports*, 536(2), 41–74. <https://doi.org/10.1016/j.physrep.2013.11.002>
- Michlmayr, G., Cohen, D., & Or, D. (2013). Shear-induced force fluctuations and acoustic emissions in granular material. *Journal of Geophysical Research: Solid Earth*, 118, 6086–6098. <https://doi.org/10.1002/2012JB009987>
- Midi, G. D. R. (2004). On dense granular flows. *European Physical Journal E*, 14(4), 341–365. <https://doi.org/10.1140/epje/i2003-10153-0>
- Murphy, K. A., Dahmen, K. A., & Jaeger, H. M. (2019). Transforming mesoscale granular plasticity through particle shape. *Physical Review X*, 9(1), 11014. <https://doi.org/10.1103/PhysRevX.9.011014>
- Nguyen, D. H., Azéma, E., Radjai, F., & Sornay, P. (2014). Effect of size polydispersity versus particle shape in dense granular media. *Physical Review E - Statistical, Nonlinear, and Soft Matter Physics*, 90(1), 1–12. <https://doi.org/10.1103/PhysRevE.90.012202>
- Nicolas, A., Ferrero, E. E., Martens, K., & Barrat, J. L. (2018). Deformation and flow of amorphous solids: Insights from elastoplastic models. *Reviews of Modern Physics*, 90(4), 45006. <https://doi.org/10.1103/RevModPhys.90.045006>
- Niiyama, T., Wakeda, M., Shimokawa, T., & Ogata, S. (2019). Structural relaxation affecting shear-transformation avalanches in metallic glasses. *Physical Review E*, 100(4), 1–10. <https://doi.org/10.1103/PhysRevE.100.043002>

- Ostojic, S., Somfai, E., & Nienhuis, B. (2006). Scale invariance and universality of force networks in static granular matter. *Nature*, *439*(7078), 828–830. <https://doi.org/10.1038/nature04549>
- Rivière, J., Lv, Z., Johnson, P. A., & Marone, C. (2018). Evolution of *b*-value during the seismic cycle: Insights from laboratory experiments on simulated faults. *Earth and Planetary Science Letters*, *482*, 407–413. <https://doi.org/10.1016/j.epsl.2017.11.036>
- Rycroft, C. H. (2009). VORO++: A three-dimensional Voronoi cell library in C++. *Chaos*. <https://doi.org/10.1063/1.3215722>
- Schofield, A., & Wroth, P. (1968). Critical state soil mechanics. *Engineer*.
- Sun, X., Kob, W., Blumenfeld, R., Tong, H., Wang, Y., & Zhang, J. (2020). *Friction-controlled entropy-stability competition in granular systems* (Vol. ii, pp. 1–5). Retrieved from <http://arxiv.org/abs/2007.14145>
- Tordesillas, A., Hilton, J. E., & Tobin, S. T. (2014). Stick-slip and force chain evolution in a granular bed in response to a grain intruder. *Physical Review E - Statistical, Nonlinear, and Soft Matter Physics*, *89*(4), 14–16. <https://doi.org/10.1103/PhysRevE.89.042207>
- Tordesillas, A., Pucilowski, S., Lin, Q., Peters, J. F., & Behringer, R. P. (2016). Granular vortices: Identification, characterization and conditions for the localization of deformation. *Journal of the Mechanics and Physics of Solids*, *90*, 215–241. <https://doi.org/10.1016/j.jmps.2016.02.032>
- Varoquaux, G., Buitinck, L., Louppe, G., Grisel, O., Pedregosa, F., & Mueller, A. (2015). Scikit-learn. *GetMobile: Mobile Computing and Communications*, *19*(1), 29–33. <https://doi.org/10.1145/2786984.2786995>
- Wang, Q., & Jain, A. (2019). A transferable machine-learning framework linking interstice distribution and plastic heterogeneity in metallic glasses. *Nature Communications*, *10*(1), 5537. <https://doi.org/10.1038/s41467-019-13511-9>
- Zhao, T., & Crosta, G. B. (2018). On the dynamic fragmentation and lubrication of coseismic landslides. *Journal of Geophysical Research: Solid Earth*, *123*, 9914–9932. <https://doi.org/10.1029/2018JB016378>
- Zheng, J., Sun, A., Wang, Y., & Zhang, J. (2018). Energy fluctuations in slowly sheared granular materials. *Physical Review Letters*, *121*(24), 248001. <https://doi.org/10.1103/PhysRevLett.121.248001>